MOLECULAR AND CELLULAR BIOLOGY, Mar. 2004, p. 2074–2082 Vol. 24, No. 5
0270-7306/04/$08.00+0 DOI: 10.1128/MCB.24.5.2074–2082.2004

Defective Neural Tube Closure and Anteroposterior Patterning in Mice Lacking the LIM Protein LMO4 or Its Interacting Partner Deaf-1

Kyungmin Hahm,[1,2]† Eleanor Y. M. Sum,[3] Yuko Fujiwara,[1] Geoffrey J. Lindeman,[3] Jane E. Visvader,[3] and Stuart H. Orkin[1,2]*

Division of Hematology-Oncology, Department of Pediatrics, Children's Hospital and Dana-Farber Cancer Institute,[1] and Howard Hughes Medical Institute,[2] Harvard Medical School, Boston, Massachusetts 02115, and VBCRC Laboratory, The Walter and Eliza Hall Institute of Medical Research, Melbourne, Victoria 3050, Australia[3]

Received 10 November 2003/Accepted 13 November 2003

LMO4 belongs to a family of transcriptional regulators that comprises two zinc-binding LIM domains. LIM-only (LMO) proteins appear to function as docking sites for other factors, leading to the assembly of multiprotein complexes. The transcription factor Deaf-1/NUDR has been identified as one partner protein of LMO4. We have disrupted the *Lmo4* and *Deaf-1* genes in mice to define their biological function in vivo. All *Lmo4* mutants died shortly after birth and showed defects within the presphenoid bone, with 50% of mice also exhibiting exencephaly. Homeotic transformations were observed in *Lmo4*-null embryos and newborn mice, but with incomplete penetrance. These included skeletal defects in cervical vertebrae and the rib cage. Furthermore, fusions of cranial nerves IX and X and defects in cranial nerve V were apparent in some $Lmo4^{-/-}$ and $Lmo4^{+/-}$ mice. Remarkably, *Deaf-1* mutants displayed phenotypic abnormalities similar to those observed in *Lmo4* mutants. These included exencephaly, transformation of cervical segments, and rib cage abnormalities. In contrast to *Lmo4* nullizygous mice, nonexencephalic *Deaf-1* mutants remained healthy. No defects in the sphenoid bone or cranial nerves were apparent. Thus, *Lmo4* and *Deaf-1* mutant mice exhibit overlapping as well as distinct phenotypes. Our data indicate an important role for these two transcriptional regulators in pathways affecting neural tube closure and skeletal patterning, most likely reflecting their presence in a functional complex in vivo.

The LIM domain is characterized by a double zinc finger structure and is found in proteins that have critical functions in cell fate determination, differentiation, and cytoskeleton organization (reviewed in references 2, 8, and 20). This motif was originally identified in LIM homeodomain transcription factors which have established roles within the central nervous system (CNS). The LIM domain also occurs in a variety of nuclear and cytoplasmic proteins, including LIM-only (LMO), LIM kinase, and focal adhesion proteins. In these proteins, there are usually two or more LIM domains, which may occur by themselves or in association with functionally divergent domains. One of the central functions of the LIM domain is to mediate protein-protein interactions, which may have either positive or negative effects on gene transcription (2, 20).

The LMO subclass of LIM proteins comprises four members (LMO1 to LMO4), each of which is defined by two tandem zinc finger domains (30). The *LMO1* and *LMO2* genes were originally identified by their translocation in acute T-cell leukemia, and their overexpression in transgenic mice leads to T-cell tumors (30). Lmo2 has been established to have a critical function in early hemopoiesis (44) and angiogenesis (43). Little is known about the physiological role of LMO3, which was cloned on the basis of sequence homology. LMO4 was identified by virtue of its interaction with the ubiquitous cofactor protein Ldb1/NLI/CLIM2 (13, 21, 33) and in an expression screen using autologous serum from a breast cancer patient (21, 31). It is the most divergent member of the family and is widely expressed in both embryonic and adult tissues, including thymus, skin, and distinct regions within the brain (6, 21, 33). The *Lmo4* gene is also highly expressed in the proliferating mammary gland and is overexpressed in more than 50% of primary breast cancers (41), underscoring its importance in the regulation of cell growth.

LMO proteins appear to function as molecular adaptors for the assembly of multiprotein complexes (30). There is no evidence that this family of LIM proteins can bind DNA specifically, but rather, their functions are primarily mediated by protein-protein interaction. LMO proteins potentially modulate transcription by binding to transcription factors or chromatin modeling proteins. LMO2 has been established to form a complex comprising the hematopoietic transcription factors SCL(TAL-1)/E2A and GATA1 as well as the cofactor Ldb1 (42). Similarly, LMO4 has been shown to participate in a novel complex comprising BRCA1 and CtIP in breast epithelial cells (34). LMO4 also associates with other proteins, including the cofactor Ldb1 (13, 21), and the transcription factors Deformed Epidermal Autoregulatory Factor-1/Nuclear Deaf Related factor (DEAF-1/NUDR/Suppressin) (33), Grainyhead-like epithelial transactivator (GET-1) (22) and the basic helix-loop-

* Corresponding author. Mailing address: Division of Hematology-Oncology, Children's Hospital and Dana-Farber Cancer Institute, Department of Pediatrics, and Howard Hughes Medical Institute, Harvard Medical School, Boston, MA 02115. Phone: (617) 632-3564. Fax: (617) 632-4367. E-mail: Stuart_Orkin@dfci.harvard.edu.

† Present address: Biogen Idec, Exploratory Science, Cambridge, MA 02142.

helix protein HEN1 (24). DEAF-1/NUDR is a nuclear DNA-binding protein that was first shown to recognize sites within the autoregulatory element of the *deformed* gene in *Drosophila melanogaster* (12). DEAF-1 comprises two conserved domains (17)—SAND (Sp100, AIRE-1, NucP41/75, DEAF-1) (4, 11) and MYND (myeloid, nervy, and deaf-1) (12), both of which are found in several transcription factors. Similar to LMO4, DEAF-1 appears to be expressed widely (17, 23). Thus, DEAF-1 and LMO4 may act as general regulators of gene transcription and may function in concert to influence biological processes in specific cell types.

To further understand the biological roles of *Lmo4* and *Deaf-1*, we have disrupted each gene by homologous recombination. We report here that mice lacking *Lmo4* die perinatally from complex phenotypic abnormalities, with approximately 50% of mice exhibiting exencephaly. *Lmo4*-deficient mice displayed defects in their presphenoid bone and cranial nerves and homeotic transformations of their cervical vertebrae and rib cage. Strikingly, *Deaf-1*-deficient mice also displayed exencephaly, skeletal anomalies, and a low frequency of homeotic transformations but no presphenoid bone or cranial nerve defects. In contrast to *Lmo4*-null mice, *Deaf-1* homozygotes that did not exhibit exencephaly survived the neonatal period and were essentially normal. Thus, *Lmo4* and *Deaf-1*-null mice exhibit both distinct and common phenotypes. The overlapping phenotypes observed in these mutant mice suggest that LMO4 and DEAF-1 form a physiological complex in specific cell types.

MATERIALS AND METHODS

Targeted disruption of the murine *Lmo4* locus. *Lmo4* genomic clones were isolated from a λFixII mouse strain 129 library (Stratagene). To generate a conditional targeting construct, a 1.0-kb *Hin*dIII fragment containing *Lmo4* 5′ DNA and a 6.0-kb *Hin*dIII-*Cla*I fragment containing 3′ DNA sequences were cloned into pTKLNCL (37). The 6.0-kb *Hin*dIII-*Cla*I fragment contains a loxP site inserted in the *Eco*RI site located 1.3 kb 3′ of the *Hin*dIII site. The targeting construct was linearized with *Kpn*I and electroporated into CJ-7 embryonic stem (ES) cells. Correctly targeted ES cell clones were injected into C57BL/6 blastocysts. To generate the *Lmo4:LacZ* knockin targeting construct, a 6.9-kb 5′ fragment was isolated; this consists of a 4.6-kb *Bam*HI-*Nco*I fragment containing the *Lmo4* 5′ flanking genomic DNA plus a 2.3-kb fragment containing the *LacZ* coding sequence followed by a poly(A) signal. This 6.9-kb fragment and a 4.7-kb *Eco*RI-*Cla*I fragment containing the *Lmo4* 3′ DNA were cloned into pTKLN, which lacks the PGK-cytosine deaminase cassette present in pTKLNCL. The targeting construct was linearized with *Sal*I and electroporated into CJ-7 ES cells. One of three targeted ES cell clones injected into C57BL/6 blastocysts gave germ line transmission. Genotyping was performed by Southern blot analysis using a 0.6-kb *Xho*I-*Hin*dIII fragment on genomic DNA digested with *Xho*I and *Eco*RV.

Targeted disruption of the murine *Deaf-1* locus. *Deaf-1* genomic clones were isolated from a RPCI-22 mouse BAC library (Research Genetics). To generate a targeting construct, a 2.8-kb *Bam*HI-*Asp*718 fragment containing *Deaf-1* 5′ DNA and a 4.1-kb *Asp*718-*Xho*I fragment containing 3′ DNA were cloned into pTKLN. The targeting construct was linearized with *Sal*I and electroporated into CJ-7 ES cells. Two independently targeted ES cell clones were injected into C57BL/6 blastocysts, one of which gave germ line transmission. Genotyping was done by Southern blot analysis using a 1.2-kb *Bgl*II-*Eco*RV fragment to probe *Bgl*II-digested genomic DNA.

Mouse breeding and embryological techniques. Chimeras were crossed with CD-1 females carrying the *Gata1-cre* transgene (18, 25) or C57BL/6 females to obtain F_1 progeny carrying the targeted *Lmo4* locus and/or *GATA1-cre* transgene. All analyses were performed with progeny from F_3 or subsequent generations. For neural crest-specific deletions, $Lmo4^{fl/fl}$ mice carrying the *Wnt1-cre* transgene were generated by mating $Lmo4^{fl/fl}$ mice with *Wnt1-cre* transgenic mice.

Whole-mount immunohistochemistry was performed on embryonic day 9.5 (E9.5) embryos using the antineurofilament antibody 2H3 (Developmental Hybridoma Bank, National Institute of Child Health and Human Development) as described by Swiatek and Gridley (35). Preparation of skeletons was as described previously (15). Briefly, embryos and mice were eviscerated, skinned, fixed in ethanol, and stained with Alcian blue or alizarin red (Sigma). Staining of embryos for *lacZ* expression was performed as described previously (25).

Immunoblot analysis. Protein lysates from wild-type and *Lmo4*-deficient E16.5 embryos were prepared in 1 ml of ice-cold lysis buffer (150 mM NaCl; 5 mM EDTA; 50 mM Tris-HCl [pH 7.5]; 1% NP-40 and 1 mM dithiothreitol, supplemented with Complete inhibitor tablet [Roche Diagnostics]; 10 mM NaF; 1 mM Na_3VO_4) from frozen embryos using a mortar and pestle. Total protein (30 μg) was denatured by boiling in sodium dodecyl sulfate loading buffer and then separated on polyacrylamide gels (Novex) prior to being transferred to polyvinylidene difluoride membranes (Millipore). Nonspecific binding of proteins to membranes was blocked by incubation in phosphate-buffered saline containing 5% skim milk and 0.1% Tween 20. The membranes were then probed with rat anti-LMO4 monoclonal antibody (1 to 2 μg/ml) or Deaf polyclonal rabbit antisera (17), a generous gift from J. Huggenvik. The membranes were subsequently incubated with horseradish peroxidase-coupled secondary antibodies (Dako) and developed by enhanced chemiluminescence (Amersham Biosciences, Inc.). To control for the integrity of proteins in tissue lysates, blots were reprobed with antitubulin monoclonal antibody (Sigma).

RESULTS

Generation of targeted *Lmo4* and *Lmo4:LacZ* knockin mice. To investigate the role of *Lmo4* during development, we used homologous recombination in ES cells to disrupt the murine *Lmo4* locus (38), which comprises three primary coding exons. We constructed a targeting vector containing three *loxP* sites flanking the first coding exon of *Lmo4* (exon 2) and the neomycin resistance cassette (Fig. 1A). Three clonal $G418^R$-targeted ES cell lines were produced, and appropriate integration was verified by Southern blot analysis using multiple probes flanking the targeted region. Chimeric mice generated from one ES cell line gave germ line transmission. These chimeras were crossed with *GATA1-cre* transgenic mice (18, 25), in which *cre* recombinase is expressed during early embryogenesis, to generate two types of mice: (i) mice in which only the neomycin resistance cassette in the *Lmo4* locus was excised (floxed allele) and (ii) mice in which both the neomycin cassette and exon 2 of the *Lmo4* gene were excised, yielding a knockout allele (Fig. 1C). Heterozygous mice were intercrossed to generate homozygous mutants. To verify that deletion of exon 2 (LIM1 domain) within the *Lmo4* locus gave rise to animals null for *Lmo4*, we performed Western blot analysis using a rat anti-LMO4 monoclonal antibody that specifically recognizes the second LIM domain of LMO4. LMO4 protein was readily detectable in E16.5 $Lmo4^{+/+}$ embryos but not in $Lmo4^{-/-}$ embryos (Fig. 1E). Thus, targeted disruption of the murine *Lmo4* gene generated a null mutation.

A *LacZ* reporter cassette was inserted into the *Lmo4* locus to allow analysis of endogenous *Lmo4* expression. The targeting vector contains the *LacZ* gene fused in frame with the translation initiation site in exon 2 of *Lmo4*; *loxP* sites were placed on either side of the *PGK-neo* selection marker cassette to allow subsequent removal (Fig. 1B). One of three correctly targeted ES cell clones, demonstrated by Southern blotting, was used to generate chimeras that underwent germ line transmission. The *neo* cassette was removed by crossing chimeric mice with transgenic mice expressing *Gata1-cre* recombinase, yielding *LacZ*/+ progeny (Fig. 1D).

Targeted disruption of the *Lmo4* gene leads to perinatal lethality and defects in neural tube closure. Although progeny

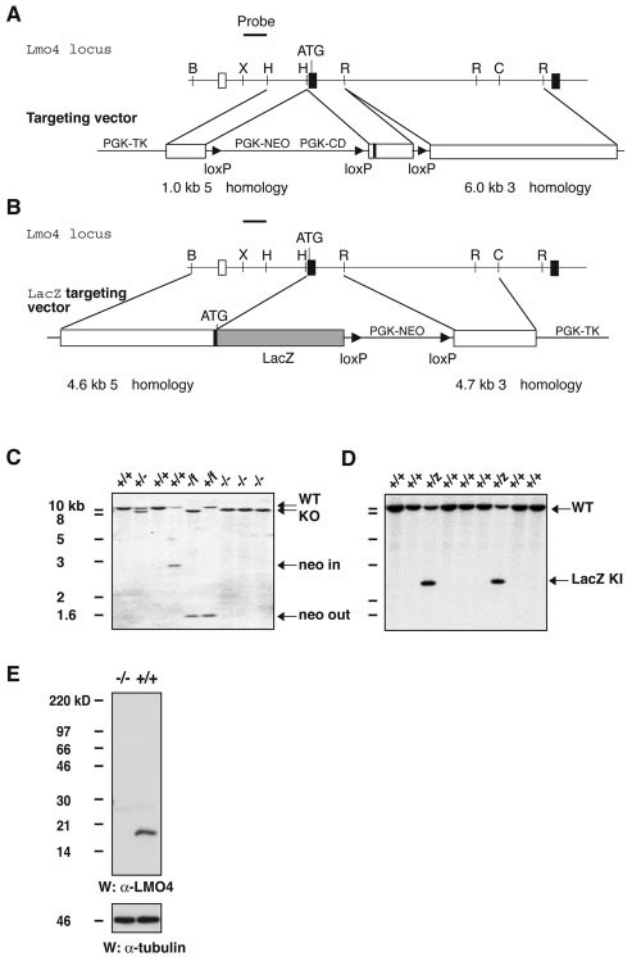

FIG. 1. Targeted disruption of the mouse *Lmo4* gene. (A) Partial restriction map of the mouse *Lmo4* gene (top) and structure of the *Lmo4* targeting vector (bottom), which contains the thymidine kinase, cytosine deaminase, and neomycin resistance (*neo*^{r}) genes, all under the control of the mouse PGK promoter. The location of the three loxP sites is given. Homologous recombination results in disruption of the coding sequence of *Lmo4* and removal of exon 2, which encodes the first LIM domain. The filled boxes represent coding exons. The flanking probe used for Southern blot analysis is shown as a black bar. (B) Structure of the *Lmo4:LacZ* knockin construct. The construct contains the *neo*^{r} and thymidine kinase genes under the control of the mouse PGK promoter. Homologous recombination results in removal of the majority of exon 2 and disruption of the coding sequence of *Lmo4*. The *LacZ* gene (shaded) was fused in frame with the translation initiation codon located at the beginning of exon 2. Exons are indicated as filled boxes. Abbreviations for restriction sites: B, *Bam*HI; RI, *Eco*RI; H, *Hin*dIII; X, *Xho*I; C, *Cla*I. (C) Generation of mice bearing either a constitutive null *Lmo4* allele or a floxed allele. Chimeras were crossed with *Gata1-cre* transgenic females to obtain F_1 progeny carrying either the floxed *Lmo4* or knockout allele. Wild-type (11-kb), knockout (10-kb; both the *neo*^{r} cassette and floxed alleles excised), floxed (1.6-kb; only the *neo* cassette excised), and wild-type but modified (2.8-kb; targeted but *neo*^{r} cassette present) alleles are indicated. Tail DNA was digested with *Xho*I and *Eco*RV, and Southern blot analysis of F_2 progeny was performed using a 600-bp *Xho*I-*Hin*dIII probe (A). (D) *Lmo4:LacZ* knockin mice were generated by breeding chimeras with *Gata1-cre* transgenic mice. Southern blot analysis of F_1 progeny was performed using DNA digested with *Eco*RV and *Xho*I and a 600-bp *Xho*I-*Hin*dIII probe. (E) Protein lysates (30 μg) from either *Lmo4*$^{-/-}$ or wild-type embryos at E16.5 were analyzed by Western blotting using a monoclonal antibody specific for the second LIM domain of Lmo4. No truncated Lmo4 protein was detected in *Lmo4*$^{-/-}$ embryos. Immunoblotting with an antitubulin antibody (α-tubulin) confirmed equal loading of protein.

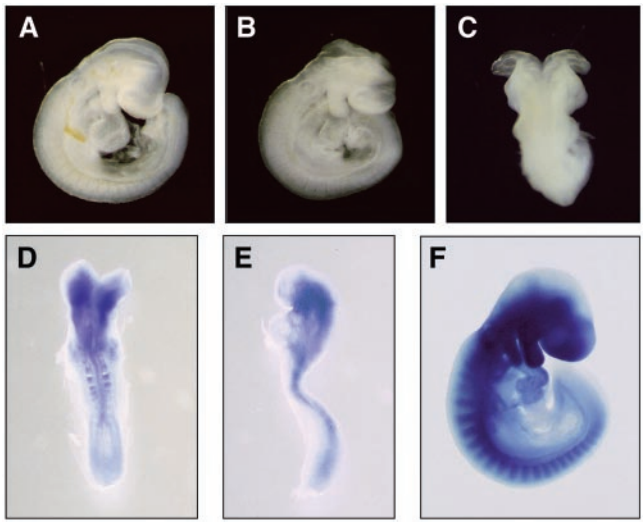

FIG. 2. Failure of neural tube closure in *Lmo4* mutants. Exencephaly was observed in approximately 50% of *Lmo4* mutants. (A to C) Wild-type (A) and mutant *Lmo4*$^{-/-}$ (B and C) embryos at E9.0 with exencephaly. (D to F) Lmo4 expression in embryos at E8.5 (D and E) and E9.5 (F), as detected by LacZ staining of *Lmo4:LacZ* knockin embryos.

were born with the expected Mendelian ratio, no *Lmo4*$^{-/-}$ neonates survived beyond the first day of birth. Among 193 live-born neonates, 45 corresponded to *Lmo4*$^{-/-}$ mice, and 23 of these were found to have exencephaly. This phenomenon results from failure of neural tube closure in the mid- and hindbrain regions during early embryogenesis (Fig. 2A to C). The majority of defects in neural tube closure affected both the mid- and hindbrain regions of *Lmo4*-null mice (Fig. 2B and C). In some cases, malformation of the hindbrain was more prominent (data not shown). Exencephaly in the *Lmo4* mutants was markedly reduced (less than 10%) on a C57BL/6 background, relative to that on a mixed (C57BL/6, CD-1, 129) background, consistent with previous findings that the exencephalic phenotype shows strain dependence (32).

All *Lmo4* mutants were born alive, including those that displayed exencephaly. Both exencephalic and nonexencephalic *Lmo4*$^{-/-}$ mice died within a few minutes of birth. *Lmo4* mutants without exencephaly gasped for air and were pale. The cause of death is unknown but may reflect failure to establish a normal breathing pattern. Histological examination of major organs within the *Lmo4*$^{-/-}$ mice did not reveal any gross morphological defects. Blood smears derived from *Lmo4* mutants demonstrated that all hematopoietic cell types were present within the normal range (data not shown).

To address whether *Lmo4* was expressed in the mid- and hindbrain regions during neural tube closure, *Lmo4:LacZ* knockin embryos were examined between E8.5 and E9.5. These mice accurately reflect the activity of the endogenous locus, as verified by immunohistochemistry using monoclonal LMO4 antibodies (unpublished data) and by RNA in situ hybridization (data not shown). In the developing mouse, the neural tube closes between E8.5 and E9.5 and is complete by late E9.5. Strong LacZ staining was evident in the mid- to hindbrain regions of E8.5 embryos as well as in the somites

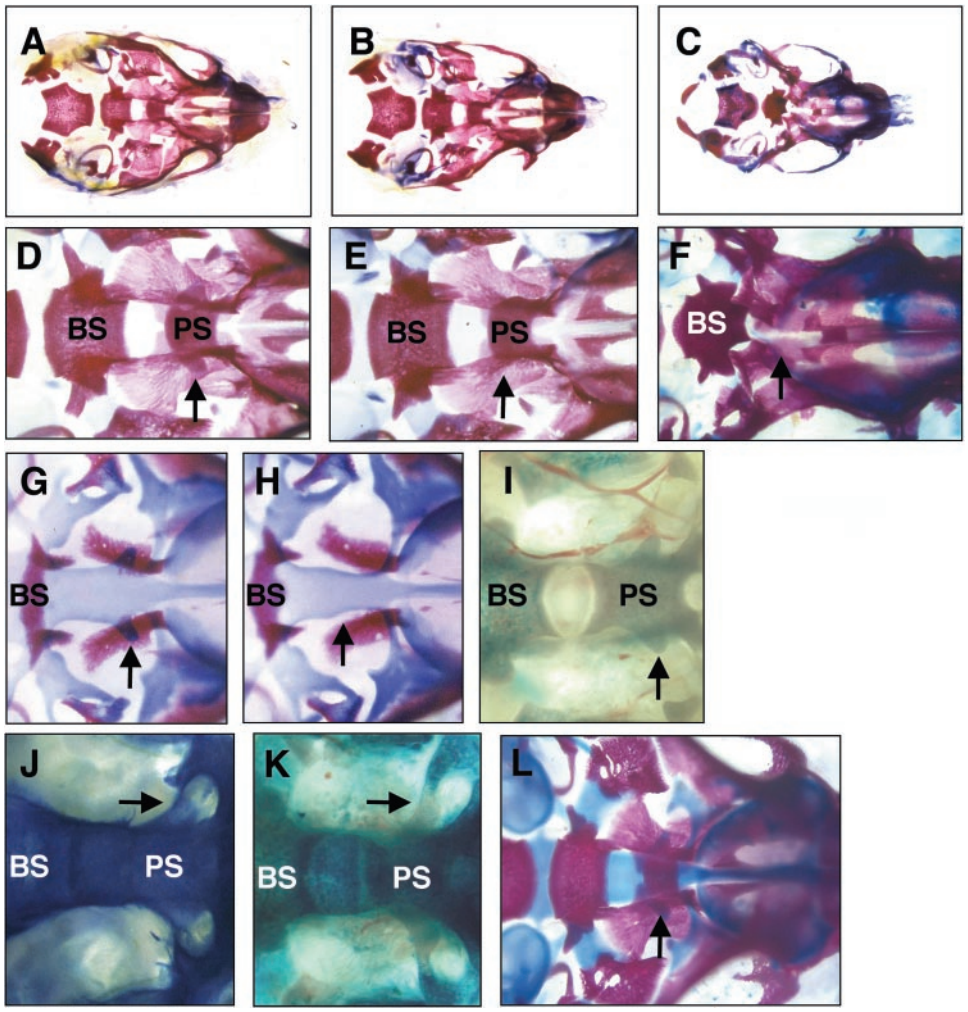

FIG. 3. Malformation of the presphenoid bone in *Lmo4* mutants. (A to F) Comparison of the internal skull base (ventral view) of wild-type mice (A and D) and newborn *Lmo4* mutants without exencephaly (B and E) and with exencephaly (C and F), following staining for bone and cartilage using alizarin red and Alcian blue. The region surrounding the sphenoid bone is shown at higher magnification in D, E, and F. The presphenoid (PS) and the basi-sphenoid (BS) bodies are fully ossified (red stain). (D) The arrow depicts the lateroposterior processes protruding from the presphenoid body; these are missing in panels E and F. (G and H) Skull bases of E16.5 wild-type and $Lmo4^{-/-}$ embryos without exencephaly, respectively. Arrows point to the region where the lateroposterior processes lie. These are missing in panel H. (I to K) Skull bases of wild-type (I), *Lmo4:LacZ* knockin heterozygote (J), and *ROSA26:LacZ*:*Wnt1-cre* (K) embryos at E18.5 were stained for LacZ activity (ventral view). The lateroposterior processes present in panel J are missing in panel K. The blue staining in panel K, in the area where the processes lie, reflects background staining from the underlying tissue. *ROSA26:LacZ*:*Wnt1-cre* reporter embryos were generated by crossing *Rosa26:LacZ* reporter mice with *Wnt1-cre* transgenic mice. (L) Alizarin red and Alcian blue staining of bone and cartilage in the presphenoid bone in $Lmo4^{fl/fl}$:*Wnt1-cre* newborn mice. The arrows mark the region where posterolateral processes protrude from the presphenoid body.

(Fig. 2D and E). In E9.5 embryos, prominent *Lmo4* expression was also observed in the brain, branchial arches, and somites (Fig. 2F), as previously reported (21, 33). Thus, *Lmo4* is expressed in the mid- and hindbrain regions at E8.5 and E9.5 when neural tube closure occurs, consistent with the observed phenotype.

Malformation of the presphenoid bone in $Lmo4^{-/-}$ mice. $Lmo4^{-/-}$ mice exhibited exencephaly with approximately 50% penetrance. In the remaining 50% of mutants, no gross defects in head structures were evident. To further investigate other potential abnormalities within the head region of both types of mutants, we examined the integrity of the skull by staining cartilage and bone. Exencephalic $Lmo4^{-/-}$ neonates displayed a profoundly malformed sphenoid bone, in which the presphenoid body was missing and the trabecula basal plate that joins the pre- and basi-sphenoid was largely missing (Fig. 3F versus D). The presphenoid body gives rise to a part of the sphenoid bone which forms the central basal plate of the skull. The presphenoid bone is first observed in the mouse embryo at approximately E15.5, as cartilage with lateral processes protruding from the posterior end of the body (Fig. 3G). By E18.5, the presphenoid body is fully ossified (Fig. 3D). In nonexencephalic *Lmo4* mutants, although the body of the presphenoid bone was present, the lateral processes originating from the posterior part of this body were missing in all embryos (eight out of eight) (Fig. 3G versus H). Examination of the presphe-

TABLE 1. Skeletal defects in *Lmo4* and *Deaf-1* mutants[a]

Genotype	Total no. of mice analyzed	No. of mice with:					
		C2/C3 fusion	Anterior tubercules	Asymmetric rib attachment	1st rib attachment	8th rib attachment	Rib bifurcation and/or fusion
Lmo4							
−/−	21	1	2 (C7)	7	0	6 (0)	0
+/−	27	0	0	4	0	1 (0)	0
+/+	17	0	0	0	0	0	0
Deaf-1							
−/−	12	0	1 (C7)	0	0	5 (2)	2
+/−	35	0	1 (C5)	1	1 (C7)	3 (0)	2
+/+	13	0	0	0	0	0	0

[a] Embryos at E18.5 and newborn mice were analyzed for skeletal defects. The numbers of mice displaying defects in their cervical vertebrae, anterior tubercules, and rib attachment following staining with alizarin red and Alcian blue are given. The location of the anterior tubercules and the number of embryos exhibiting bilateral eighth-rib attachment are shown in parentheses.

noid body in E15.5 to E17.5 $Lmo4^{-/-}$ embryos demonstrated that these processes did not appear as cartilage primordia at E16.5 (Fig. 3H) and had failed to form by E17.5 (data not shown). Thus, malformation of the presphenoid bone in these *Lmo4* mutants is likely to stem from improper formation of cartilage at E16.5. In normal animals, the cartilage within these lateral processes undergoes ossification and eventually contributes to the lateral walls of the optic canals, through which the optic fibers pass. In *Lmo4* mutants (both E18.5 embryos and newborn mice), the inferior half of the lateral optic canal did not form properly and muscle and ligamentous attachments in this region were disorganized (data not shown).

To examine the expression of the *Lmo4* gene in presphenoid and sphenoid bones, we analyzed *Lmo4:LacZ* knockin embryos between E15.5 and E18.5. Significantly, *Lmo4* was expressed in most of the bones within the skull, including the sphenoid and occipital bones. *Lmo4* promoter activity was clearly evident within the presphenoid bone and in the extending processes from E15.5 (data not shown) to E18.5 (Fig. 3J), where defects in bone formation occur. To determine whether the presphenoid processes missing in *Lmo4* mutants were derived from neural crest cells, we crossed *Wnt1-cre* transgenic mice (5, 7) with $Lmo4^{fl/fl}$ or $Lmo4^{-/fl}$ mice. *Wnt1* regulatory sequences direct expression in premigratory neural crest cells derived from the dorsal CNS and demarcate the presumptive midbrain (9). We first characterized the expression pattern of *Wnt1-cre* in the skull base using *ROSA26:LacZ* reporter mice (25). β-Galactosidase activity was not detected in the lateral processes of the presphenoid (Fig. 3K). However, other areas of the sphenoid body showed definitive LacZ staining, demonstrating that neural crest cells contribute to the sphenoid bone. In $LMO4^{fl/fl}$:*Wnt1-cre* newborn mice, the presphenoid bone formed properly and was identical to that seen in wild-type mice (Fig. 3L). This finding is consistent with our data indicating that the lateral wings may not originate from the neural crest lineage.

***Lmo4* mutant mice exhibit homeotic-like transformations in their rib cage and cervical vertebrae.** LMO proteins and their cofactor Ldb-1 have been implicated in regulating the transcriptional activity of various homeobox proteins, via either direct or indirect interactions with these proteins (2, 20). We explored whether *Lmo4* mutant mice manifested any patterning defects reminiscent of those that occur in *Hox*-deficient mice. The skeletons of wild-type, $Lmo4^{+/-}$, and $Lmo4^{-/-}$ mice were stained with alizarin red and Alcian blue, which are specific for bone and cartilage, respectively. Table 1 summarizes the homeotic-like transformations observed in *Lmo4* mutants (E18.5 embryos and newborn mice). A variety of malformations and segment identity defects were observed in both $Lmo4^{-/-}$ and $Lmo4^{+/-}$ mice, but with variable penetrance. $Lmo4^{-/-}$ mice (6 of 21) displayed defects in their rib cage, in which the eighth rib was aberrantly attached to the sternum (Fig. 4A versus B). Most of the attachment occurred on the right side, but two embryos were noted to have the eighth rib attached to the sternum on both sides, resulting in bilateral rib attachment (data not shown). One *Lmo4* heterozygote also showed attachment of the eighth rib to the sternum. Asymmetric attachment, i.e., disorganized attachment of ribs to the sternum, was frequently observed in *Lmo4* mutants (Fig. 4C versus D; Table 1): 7 out of 21 $Lmo4^{-/-}$ and 4 out of 27 $Lmo4^{+/-}$ mice. In severe cases, the first rib was not attached to the body of the sternum. In addition to defects within the rib cage, *Lmo4* mutants displayed infrequent homeotic transformations of their cervical vertebrae. Furthermore, in 2 out of 21 embryos, the anterior tubercule was found attached to C7 instead of C6 (Fig. 4E versus F). Partial fusion of C2 and C3 vertebrae was observed in one *Lmo4* mutant (Fig. 4G).

***Lmo4*-null mice exhibit cranial nerve defects.** Since *Lmo4* is highly expressed in the CNS and spinal column, we investigated possible defects in cranial nerve patterning. Staining of *Lmo4* mutant embryos at E9.5 for neurofilaments showed that frequent fusion of cranial nerves IX and X occurred in mutant (50% of mutants) but not wild-type embryos (Fig. 5A versus C and D). This defect was also apparent in approximately 25% of *Lmo4* heterozygous embryos, suggesting haploinsufficiency (Fig. 5B). Furthermore, defects in cranial nerve V were found in 20% of embryos examined. In these embryos, a segment of cranial nerve V that migrates to branchial arch 2 was missing. In addition, the connection between ganglion and rhombomere r2 exit points appeared to be greatly reduced or missing in these embryos (Fig. 5D). Migration of cranial nerve V to the first branchial arch, however, was normal.

Targeted disruption of the murine *Deaf-1* gene leads to neural tube defects and skeletal abnormalities. LMO4 has been shown to associate with the DNA-binding protein Deaf-1,

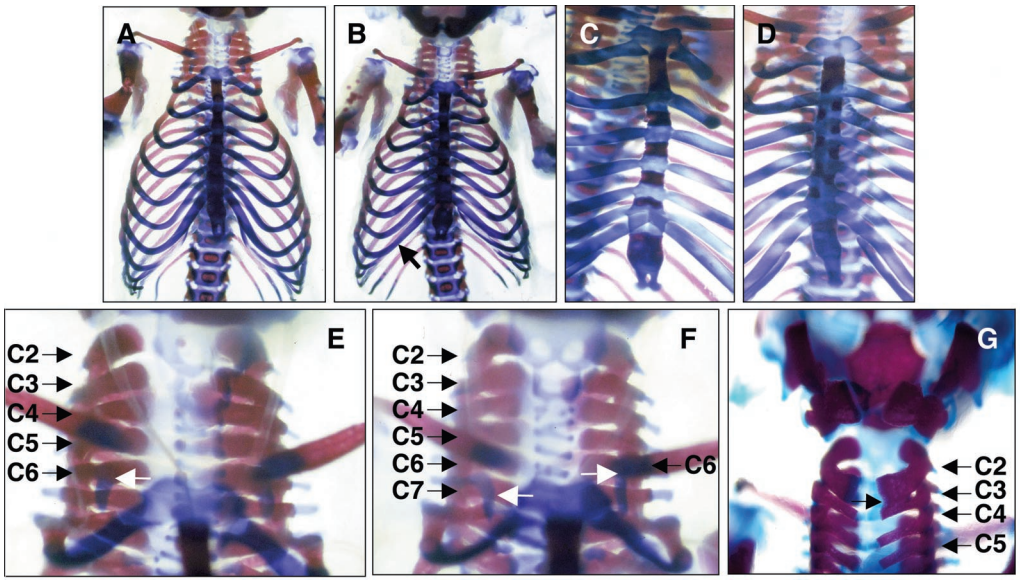

FIG. 4. Skeletal abnormalities in *Lmo4* mutant mice. Bone and cartilage were stained with alizarin red and Alcian blue, respectively. (A to D) Ventral view of sternum and ribcage in wild-type mice (A and C) and *Lmo4* mutants (B and D). (B) Aberrant attachment of the eighth rib to the sternum is indicated by a solid arrow. (D) Asymmetric alignment of the ribs is shown. (C) Symmetric alignment occurs in wild-type mice. In some *Lmo4* mutants (F), anterior tubercules (AT) were attached to C7 (F) instead of C6, as occurs in wild-type mice (E). (F) One AT appears to be attached to both C6 and C7. (G) In another Lmo4 mutant, partial fusion of C2 and C3 was observed. AT stained with Alcian blue are indicated by white arrows. Vertebrae C2 to C7 are indicated by arrows.

both of which are widely expressed throughout adult tissues (33). To assess the potential role of *Deaf-1* in development and any overlap in phenotype between *Lmo4* and *Deaf-1* mutants, we generated targeted mice using homologous recombination in ES cells. The targeting construct was designed to delete two exons (amino acids 192 to 269) encoding the SAND DNA-binding domain (4, 11), by replacing it with a *PGK-neo* cassette, flanked by *loxP* sites (Fig. 6A). Three clones underwent appropriate recombination, as determined by Southern analysis using different probes, and were used to generate chimeras. The *PGK-neo* selection cassette was excised by mating with *Gata1-cre* transgenic mice. A representative Southern blot of F_1 progeny is shown in Fig. 6B. Mice heterozygous for the *Deaf-1* locus were interbred to generate homozygous mice. Immunoblotting of protein lysates from wild-type and *Deaf-1* mutant embryos using anti-Deaf-1 polyclonal antisera verified that the *Deaf-1* locus had been disrupted (Fig. 6C).

Offspring with wild-type, heterozygous, and homozygous genotypes were represented in Mendelian proportions. Similar to *Lmo4* mutant mice, some *Deaf-1* mutants exhibited exencephaly at birth. Of 55 embryos at E18.5, 9 out of 11 *Deaf-1*$^{-/-}$ mutants showed defects in neural tube closure (Fig. 7A versus B). The penetrance was observed to be higher in *Deaf-1* than *Lmo4* mutants, with 80% affected on a mixed genetic background. Exencephalic mice died shortly after birth, whereas *Deaf-1* mutants without exencephaly were healthy and fertile and did not display any gross abnormalities. A significant proportion of *Deaf-1* heterozygous animals (30%; 9 of 30 mice) also showed exencephaly, most likely reflecting haploinsufficiency. Interestingly, no abnormalities in the sphenoid bone were observed, in contrast with findings in *Lmo4* mutants.

Deaf-1 mutants showed skeletal abnormalities in the rib cage and in their cervical vertebrae, reminiscent of defects in *Lmo4*-null embryos. In the rib cage, improper attachment of the eighth rib to the sternum was observed in 5 out of 12 embryos at E18.5 (Fig. 7D), whereas this did not occur in wild-type embryos (Fig. 7C). In addition, 2 out of 12 *Deaf-1*$^{-/-}$ and 2 out of 35 *Deaf-1*$^{+/-}$ mice displayed bifurcated or fused ribs. A *Deaf-1* heterozygous embryo showing bifurcation and fusion of the eighth and ninth ribs is depicted in Fig. 7E. Both homozygous and heterozygous *Deaf-1* mice displaying fusion of the first and second ribs also showed aberrant attachment of anterior tubercules to cervical vertebrae (Fig. 7F and G). In one *Deaf-1*$^{-/-}$ embryo, the anterior tubercule was attached to C7 instead of C6, whereby C7 acquired the identity of C6 (Fig. 7F). In a *Deaf-1*$^{+/-}$ embryo, the anterior tubercule was attached to C5, manifest as a C5-to-C6 transformation (Fig. 7G). In addition, this *Deaf-1*$^{+/-}$ embryo showed aberrant attachment of the first rib to C7 rather than to T1. Thus, in this embryo, posteriorization of the region from C5 to C7 has occurred. Interestingly, *Deaf-1* mutant embryos did not show any defects in cranial nerve patterning, in contrast with that observed in *Lmo4* mutant embryos.

DISCUSSION

Members of the *Lmo* family of transcriptional coregulators have distinct expression profiles. *Lmo4*, the fourth member of this class, is widely expressed throughout embryonic development and in adult tissues. In contrast, *Lmo1*, *Lmo2*, and *Lmo3* exhibit patterns of expression that are more tissue restricted. Within the embryo, *Lmo4* is predominantly expressed in the CNS and peripheral nervous system, the thymus, the epidermis, and other epithelial tissues (21, 33). In the adult, high mRNA levels are found in brain, thymus, heart, mammary

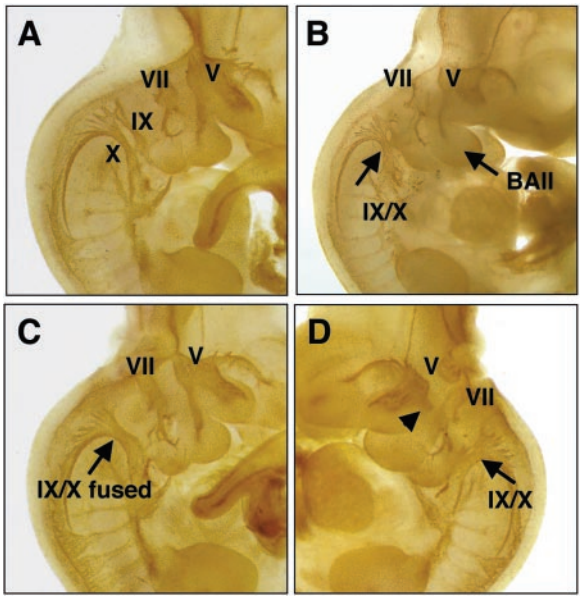

FIG. 5. Cranial nerve malformation in *Lmo4* mutant embryos. Wild-type (A), heterozygous (B), and homozygous *Lmo4* (C and D) embryos at E9.5 were stained for neurofilaments using antibody 2H2. Fusion of cranial nerves IX and X, which occurs in 50% of $Lmo4^{-/-}$ and 25% of $Lmo4^{+/-}$ embryos, is indicated by arrows. In 2 out of 10 $Lmo4^{-/-}$ embryos, abnormal staining of axons surrounding ganglion V was observed (arrowhead in panel D). Cranial nerves V, VII, IX, and X and branchial arch II (BAII) are indicated.

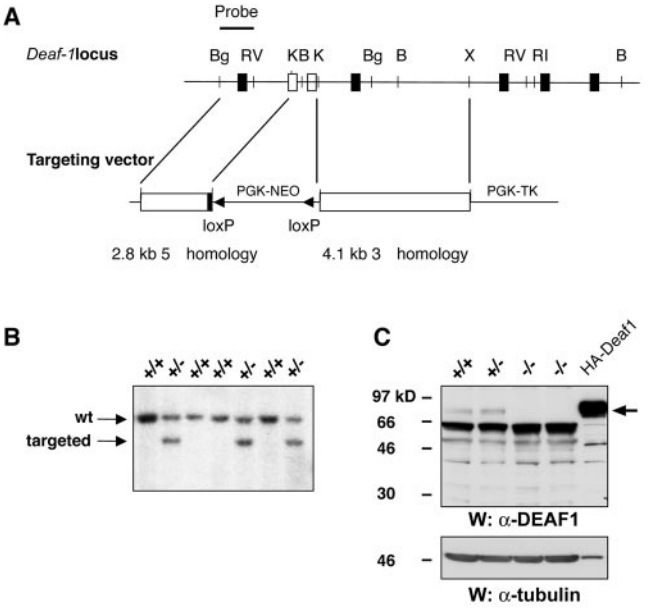

FIG. 6. Targeted disruption of the mouse *Deaf-1* gene. (A) Partial restriction map of the mouse *Deaf-1* gene (top) and structure of the *Deaf-1* targeting vector (bottom), which contains the thymidine kinase and neomycin resistance (*neo*^{r}) genes, both under the control of the mouse PGK promoter. Homologous recombination results in disruption of two exons encoding the SAND domain, represented as open boxes. The flanking probe used for Southern blot analysis is shown as a black bar. Abbreviations for restriction sites: Bg, *Bgl*II; B, *Bam*HI; K, *Asp*718; R1, *Eco*RI; X, *Xho*I. (B) Generation of $Deaf\text{-}1^{+/-}$ mice. *Deaf-1* chimeras were crossed with *Gata1-cre* transgenic mice to generate F_1 progeny heterozygous for the targeted *Deaf-1* allele. DNA was digested with *Eco*RI, and Southern blot analysis was performed using the 1.2-kb *Bgl*II-*Eco*RV probe indicated in panel A. (C) Protein lysates (30 μg) derived from E16.5 embryos were analyzed by Western blotting using a polyclonal antibody raised against Deaf-1. No Deaf-1 protein was observed in $Deaf\text{-}1^{-/-}$ embryos. The faint band at 46 kDa appears in both wild-type and −/− embryonic extracts and represents a nonspecific cross-reactive product. 293T cells transfected with an expression vector encoding hemagglutinin-tagged Deaf-1 served as a control. Western blot analysis using antitubulin antibody (α-tubulin) confirmed equal loading.

gland, skin, lung, liver, and spleen (21, 31, 33, 41). We report here that targeted disruption of the murine *Lmo4* gene leads to early neonatal lethality. Multiple defects were evident in these mice, including failure of the neural tube to close, sphenoid bone abnormalities, and aberrant skeletal patterning. No anomalies were apparent in the major organs or within the hemopoietic compartment. Despite prominent expression of *Lmo4* in lymphocytes, no defects were found in the ability of $Lmo4^{-/-}$ ES cells to reconstitute the lymphoid compartment of *Rag2*-deficient mice (unpublished data).

Strikingly, exencephaly and homeotic transformations were also observed in mice lacking Deaf-1, a transcription factor that has been demonstrated to interact directly with Lmo4. *Deaf-1*, like *Lmo4*, displays a wide tissue distribution in adult tissues, including brain, lung, and skin (17, 23). This factor comprises a SAND domain with a conserved KDWK core that mediates DNA binding and a MYND domain consisting of a potential zinc-binding motif involved in protein-protein interactions. In *Drosophila*, *Deaf-1* has been established to be essential for early embryonic development (39). Arrest usually occurred prior to zygotic gene expression, but some embryos developed into larvae that exhibited segmentation defects with variable severity. These defects included loss of segments and abnormal segment development along the anterior-posterior axis.

Lmo4 and *Deaf-1* mutant mice exhibit common as well as distinct phenotypes. Both genes appear to be required for closure of the neural tube. Fifty percent of *Lmo4* mutants exhibited exencephaly, while up to 80% of *Deaf-1*-deficient mice showed this defect. Unlike *Deaf-1* mice, *Lmo4* mutants without exencephaly died within a few minutes of birth. In the developing mouse, high levels of *Lmo4* mRNA are present within neural crest cells, in addition to motor neurons, sensory neurons, somites, and Schwann cell progenitors (6, 21, 33). Specific targeting of the *Lmo4* gene in either neural crest lineage cells or neuronal cells within the CNS, using *Wnt1-cre* or *Nestin-cre* transgenic mice, respectively, led to perinatal lethality or growth retardation (data not shown). Thus, while it is not clear what the underlying causes of neonatal lethality are, it is apparent that *Lmo4* expression is required in these cell derivatives for proper development. *Lmo4* but not *Deaf-1* mutant mice showed abnormalities in the sphenoid bone at the base of the skull with complete penetrance. The lateral processes emanating from the presphenoid body were absent in *Lmo4* homozygous mice, and in exencephalic *Lmo4* mutants both the presphenoid body and trabecula basal plate were apparently missing. The biological consequences of these defects are not well understood.

Lmo4 and *Deaf-1* mutant mice exhibit defects in their cer-

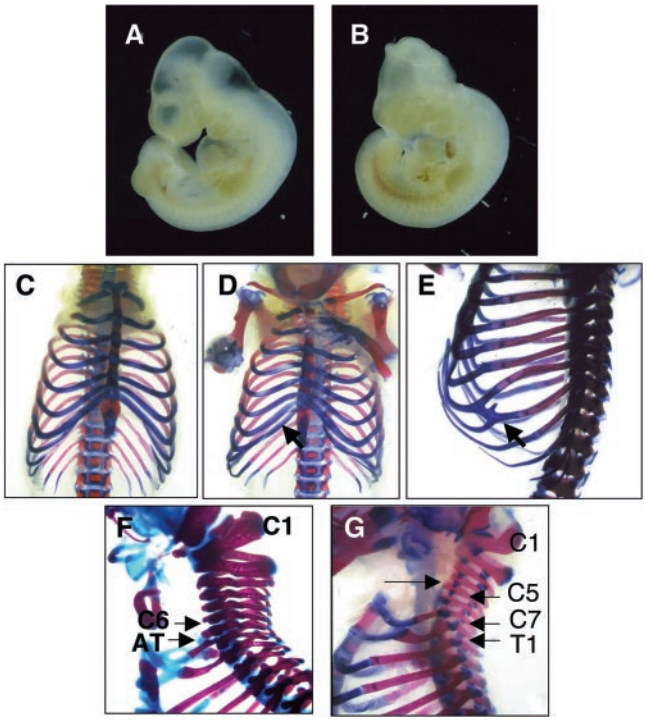

FIG. 7. Defective neural tube closure and skeletal abnormalities in *Deaf-1*-deficient embryos. *Deaf-1* mutant embryos (B) fail to close their neural tube by E10.5 and show outgrowth of the mid-hindbrain region compared to wild-type embryos (A). The penetrance of this phenotype on a mixed genetic background was 80%. (C to G) Bone and cartilage of wild-type (C) and *Deaf-1* mutants (D to G) were stained with alizarin red and Alcian blue to analyze potential skeletal defects. Five out of twelve *Deaf-1* mutants showed attachment of the eighth rib to the sternum (D) as seen in *Lmo4* mutants. Two out of 35 *Deaf-1*$^{+/-}$ (E and G) and 2 out of 12 *Deaf-1*$^{-/-}$ (F) embryos showed bifurcation or fusion of ribs. The eighth and ninth ribs were bifurcated (E), while the first and second ribs appeared to be fused, as indicated by the arrows (F and G). Only one *Deaf-1*$^{-/-}$ embryo (F) showed fusion of the first and second ribs, and the anterior tubercule (AT) was attached to C7 instead of C6, as indicated by the arrow. In a *Deaf-1* heterozygote (G), the first rib was attached to C7 instead of T1 and the AT was attached to C5 instead of C6.

vical vertebrae and rib cage. In addition, some of the transformations evident in *Lmo4* and *Deaf-1* mutants affected both homozygotes and heterozygotes, suggesting that gene dosage is important for correct function. In both *Lmo4* and *Deaf-1* mutants, the eighth rib was found aberrantly attached to the sternum. Asymmetric attachment of ribs was visualized frequently in *Lmo4*-null mice but rarely in *Deaf-1* mutants. Conversely, bifurcated ribs were noted in *Deaf-1* mutants but not in *Lmo4*-deficient mice. Transformations of cervical vertebrae were observed infrequently in both *Lmo4* and *Deaf-1* mutants. In contrast, cranial nerve defects in the hindbrain region were only evident in *Lmo4* mutants. This probably arises from improper boundary formation within rhombomeres, caused by defective neuronal pathfinding. It is possible that *Lmo4* plays a role in axon pathfinding in the hindbrain, similar to that of *Hoxa2* (10).

The transformations observed in *Lmo4* and *Deaf-1* mutants and the cranial nerve defects evident in *Lmo4* mutants are frequently seen in *Hox*-deficient mice, suggesting that *Lmo4* and/or *Deaf-1* alters the expression or activity of these homeobox proteins. Multiple genes within paralogous *Hox* groups 3 and 4 exhibit complex rib attachment and sternum phenotypes in knockout mice. Moreover, several *Hox* genes (such as *Hoxa2*, *Hoxa3*, and *Hoxb3*) expressed in the anterior boundary of the hindbrain lead to defects in cranial nerve patterning when disrupted (36). Hox transcription factor genes may represent targets of Lmo4 and Deaf-1. Alternatively, Lmo4/Deaf-1 may act as cofactors for Hox proteins and influence their activity. In the latter case, a shift in Hox gene expression would not be expected in either *Lmo4* or *Deaf-1* mutants, but rather, the ability of specific Hox factors to activate or repress their target genes would be altered. Deaf-1 was originally identified as a cofactor for the Hox protein Deformed, which is required for the development of structures derived from the mandibular and maxillary segments in *Drosophila* (27). It is tempting to speculate that Deaf-1 (and Lmo4) plays a parallel role as a Hox cofactor in mammals. Interestingly, Ldb1, a cofactor for Lmo4 and other LIM domain proteins, has been shown to bind and/or influence the function of Hox proteins, including Otx, Bicoid, and ftz, and the LIM homeodomain proteins Lhx1, Lhx3, and Lmx, (1, 3, 14, 19, 28). Removal of the mouse *Ldb1* gene leads to early embryonic lethality associated with multiple patterning defects during gastrulation, including truncation of the anterior-to-hindbrain structures (29). Some of these phenotypes may be mediated via Hox or other homeodomain proteins. Taken together, it seems likely that the presumptive Lmo4/Deaf-1 or Lmo4/Deaf-1/Ldb1 complexes play a role in modulating Hox function in specific cell types.

Both *Lmo4* and *Deaf-1* mutants demonstrate homeotic-like transformations that vary in penetrance. Indeed, many of the homeotic transformations in single *Hox* mutants exhibit low penetrance and variable expression until compound targeted mice are generated. For example, targeted deletion of all *HoxB* genes results in a more penetrant and severe phenotype that represents the sum of those observed in single *HoxB* gene mutants (26). In addition, compound mutants for paralogous group genes (Hoxa-4, Hoxb-4, and Hoxd-4) show more complete homeotic transformations and a dose-dependent increase in the number of transformed vertebrae relative to that in single mutants (16).

There is increasing evidence that LMO-mediated interactions have functional relevance. Lmo2 has been established to form multiprotein transcriptional complexes in vivo with the hemopoietic transcription factors Scl/Tal-1 and Gata-1 and the ubiquitous regulators E47 and Ldb1 (42). Biochemical analyses of hematopoietic nuclear extracts has provided further evidence that these high-molecular-weight complexes exist (40). Mice deficient in *Lmo2*, *Scl*, and *Gata-1* have established a close functional relationship between these proteins in the hematopoietic system. The skeletal transformations and defective neural tube closure reported here for the *Lmo4* and *Deaf-1* mutants suggest that Lmo4 and Deaf-1 form a physiological protein complex in specific cell types. The distinct phenotypes apparent in *Lmo4* mutants further reveal that *Lmo4* possesses *Deaf-1*-independent functions. Elucidation of the targets of Lmo4 and Deaf-1 should provide insight into the molecular mechanisms underlying the complex phenotypic abnormalities observed in *Lmo4*- and *Deaf-1*-null mice.

ACKNOWLEDGMENTS

We thank R. Bronson for histologic examination of *Lmo4*$^{-/-}$ sections, A. McMahon for Wnt1-cre transgenic mice, and J. Huggenvik for NUDR antibody. We are grateful to A. Voss for critical review of the manuscript.

J.V., G.L., and E.S. were supported by the Victorian Breast Cancer Research Consortium, Melbourne, Australia.

REFERENCES

1. **Agulnick, A. D., M. Taira, J. J. Breen, T. Tanaka, I. B. Dawid, and H. Westphal.** 1996. Interactions of the LIM-domain-binding factor Ldb1 with LIM homeodomain proteins. Nature **384:**270–272.
2. **Bach, I.** 2000. The LIM domain: regulation by association. Mech. Dev. **91:**5–17.
3. **Bach, I., C. Carriere, H. P. Ostendorff, B. Andersen, and M. G. Rosenfeld.** 1997. A family of LIM domain-associated cofactors confer transcriptional synergism between LIM and Otx homeodomain proteins. Genes Dev. **11:** 1370–1380.
4. **Bottomley, M. J., M. W. Collard, J. I. Huggenvik, Z. Liu, T. J. Gibson, and M. Sattler.** 2001. The SAND domain structure defines a novel DNA-binding fold in transcriptional regulation. Nat. Struct. Biol. **8:**626–633.
5. **Chai, Y., X. Jiang, Y. Ito, P. Bringas, Jr., J. Han, D. H. Rowitch, P. Soriano, A. P. McMahon, and H. M. Sucov.** 2000. Fate of the mammalian cranial neural crest during tooth and mandibular morphogenesis. Development **127:**1671–1679.
6. **Chen, H. H., J. W. Yip, A. F. Stewart, and E. Frank.** 2002. Differential expression of a transcription regulatory factor, the LIM domain only 4 protein Lmo4, in muscle sensory neurons. Development **129:**4879–4889.
7. **Danielian, P. S., D. Muccino, D. H. Rowitch, S. K. Michael, and A. P. McMahon.** 1998. Modification of gene activity in mouse embryos in utero by a tamoxifen-inducible form of Cre recombinase. Curr. Biol. **8:**1323–1326.
8. **Dawid, I. B., J. J. Breen, and R. Toyama.** 1998. LIM domains: multiple roles as adapters and functional modifiers in protein interactions. Trends Genet. **14:**156–162.
9. **Echelard, Y., G. Vassileva, and A. P. McMahon.** 1994. Cis-acting regulatory sequences governing Wnt-1 expression in the developing mouse CNS. Development **120:**2213–2224.
10. **Gavalas, A., M. Davenne, A. Lumsden, P. Chambon, and F. M. Rijli.** 1997. Role of Hoxa-2 in axon pathfinding and rostral hindbrain patterning. Development **124:**3693–3702.
11. **Gibson, T. J., C. Ramu, C. Gemund, and R. Aasland.** 1998. The APECED polyglandular autoimmune syndrome protein, AIRE-1, contains the SAND domain and is probably a transcription factor. Trends Biochem. Sci. **23:**242–244.
12. **Gross, C. T., and W. McGinnis.** 1996. DEAF-1, a novel protein that binds an essential region in a Deformed response element. EMBO J. **15:**1961–1970.
13. **Grutz, G., A. Forster, and T. H. Rabbitts.** 1998. Identification of the LMO4 gene encoding an interaction partner of the LIM-binding protein LDB1/NLI1: a candidate for displacement by LMO proteins in T cell acute leukaemia. Oncogene **17:**2799–2803.
14. **Hobert, O., and H. Westphal.** 2000. Functions of LIM-homeobox genes. Trends Genet. **16:**75–83.
15. **Hogan, B., R. Beddington, F. Costantini, and E. Lucy.** 1994. Manipulating the mouse embryo. Cold Spring Harbor Laboratory Press, Plainview, N.Y.
16. **Horan, G. S., R. Ramirez-Solis, M. S. Featherstone, D. J. Wolgemuth, A. Bradley, and R. R. Behringer.** 1995. Compound mutants for the paralogous hoxa-4, hoxb-4, and hoxd-4 genes show more complete homeotic transformations and a dose-dependent increase in the number of vertebrae transformed. Genes Dev. **9:**1667–1677.
17. **Huggenvik, J. I., R. J. Michelson, M. W. Collard, A. J. Ziemba, P. Gurley, and K. A. Mowen.** 1998. Characterization of a nuclear deformed epidermal autoregulatory factor-1 (DEAF-1)-related (NUDR) transcriptional regulator protein. Mol. Endocrinol. **12:**1619–1639.
18. **Jasinski, M., P. Keller, Y. Fujiwara, S. H. Orkin, and M. Bessler.** 2001. GATA1-Cre mediates Piga gene inactivation in the erythroid/megakaryocytic lineage and leads to circulating red cells with a partial deficiency in glycosyl phosphatidylinositol-linked proteins (paroxysmal nocturnal hemoglobinuria type II cells). Blood **98:**2248–2255.
19. **Jurata, L. W., and G. N. Gill.** 1997. Functional analysis of the nuclear LIM domain interactor NLI. Mol. Cell. Biol. **17:**5688–5698.
20. **Jurata, L. W., and G. N. Gill.** 1998. Structure and function of LIM domains. Curr. Top. Microbiol. Immunol. **228:**75–113.
21. **Kenny, D. A., L. W. Jurata, Y. Saga, and G. N. Gill.** 1998. Identification and characterization of LMO4, an LMO gene with a novel pattern of expression during embryogenesis. Proc. Natl. Acad. Sci. USA **95:**11257–11262.
22. **Kudryavtseva, E. I., T. M. Sugihara, N. Wang, R. J. Lasso, J. F. Gudnason, S. M. Lipkin, and B. Andersen.** 2003. Identification and characterization of Grainyhead-like epithelial transactivator (GET-1), a novel mammalian Grainyhead-like factor. Dev. Dyn. **226:**604–617.
23. **LeBoeuf, R. D., E. M. Ban, M. M. Green, A. S. Stone, S. M. Propst, J. E. Blalock, and J. D. Tauber.** 1998. Molecular cloning, sequence analysis, expression, and tissue distribution of suppressin, a novel suppressor of cell cycle entry. J. Biol. Chem. **273:**361–368.
24. **Manetopoulos, C., A. Hansson, J. Karlsson, J. I. Jonsson, and H. Axelson.** 2003. The LIM-only protein LMO4 modulates the transcriptional activity of HEN1. Biochem. Biophys. Res. Commun. **307:**891–899.
25. **Mao, X., Y. Fujiwara, and S. H. Orkin.** 1999. Improved reporter strain for monitoring Cre recombinase-mediated DNA excisions in mice. Proc. Natl. Acad. Sci. USA **96:**5037–5042.
26. **Medina-Martinez, O., A. Bradley, and R. Ramirez-Solis.** 2000. A large targeted deletion of Hoxb1-Hoxb9 produces a series of single-segment anterior homeotic transformations. Dev. Biol. **222:**71–83.
27. **Merrill, V. K., F. R. Turner, and T. C. Kaufman.** 1987. A genetic and developmental analysis of mutations in the Deformed locus in Drosophila melanogaster. Dev. Biol. **122:**379–395.
28. **Mochizuki, T., A. A. Karavanov, P. E. Curtiss, K. T. Ault, N. Sugimoto, T. Watabe, K. Shiokawa, M. Jamrich, K. W. Cho, I. B. Dawid, and M. Taira.** 2000. Xlim-1 and LIM domain binding protein 1 cooperate with various transcription factors in the regulation of the goosecoid promoter. Dev. Biol. **224:**470–485.
29. **Mukhopadhyay, M., A. Teufel, T. Yamashita, A. D. Agulnick, L. Chen, K. M. Downs, A. Schindler, A. Grinberg, S. P. Huang, D. Dorward, and H. Westphal.** 2003. Functional ablation of the mouse Ldb1 gene results in severe patterning defects during gastrulation. Development **130:**495–505.
30. **Rabbitts, T. H.** 1998. LMO T-cell translocation oncogenes typify genes activated by chromosomal translocations that alter transcription and developmental processes. Genes Dev. **12:**2651–2657.
31. **Racevskis, J., A. Dill, J. A. Sparano, and H. Ruan.** 1999. Molecular cloning of LMO4, a new human LIM domain gene. Biochim. Biophys. Acta **1445:** 148–153.
32. **Sah, V. P., L. D. Attardi, G. J. Mulligan, B. O. Williams, R. T. Bronson, and T. Jacks.** 1995. A subset of p53-deficient embryos exhibit exencephaly. Nat. Genet. **10:**175–180.
33. **Sugihara, T. M., I. Bach, C. Kioussi, M. G. Rosenfeld, and B. Andersen.** 1998. Mouse deformed epidermal autoregulatory factor 1 recruits a LIM domain factor, LMO-4, and CLIM coregulators. Proc. Natl. Acad. Sci. USA **95:**15418–15423.
34. **Sum, E. Y., B. Peng, X. Yu, J. Chen, J. Byrne, G. J. Lindeman, and J. E. Visvader.** 2002. The LIM domain protein LMO4 interacts with the cofactor CtIP and the tumor suppressor BRCA1 and inhibits BRCA1 activity. J. Biol. Chem. **277:**7849–7856.
35. **Swiatek, P. J., and T. Gridley.** 1993. Perinatal lethality and defects in hindbrain development in mice homozygous for a targeted mutation of the zinc finger gene Krox20. Genes Dev. **7:**2071–2084.
36. **Trainor, P. A., and R. Krumlauf.** 2000. Patterning the cranial neural crest: hindbrain segmentation and Hox gene plasticity. Nat. Rev. Neurosci. **1:**116–124.
37. **Tsang, A. P., Y. Fujiwara, D. B. Hom, and S. H. Orkin.** 1998. Failure of megakaryopoiesis and arrested erythropoiesis in mice lacking the GATA-1 transcriptional cofactor FOG. Genes Dev. **12:**1176–1188.
38. **Tse, E., G. Grutz, A. A. Garner, Y. Ramsey, N. P. Carter, N. Copeland, D. J. Gilbert, N. A. Jenkins, A. Agulnick, A. Forster, and T. H. Rabbitts.** 1999. Characterization of the Lmo4 gene encoding a LIM-only protein: genomic organization and comparative chromosomal mapping. Mamm. Genome **10:** 1089–1094.
39. **Veraksa, A., J. Kennison, and W. McGinnis.** 2002. DEAF-1 function is essential for the early embryonic development of Drosophila. Genesis **33:** 67–76.
40. **Visvader, J. E., X. Mao, Y. Fujiwara, K. Hahm, and S. H. Orkin.** 1997. The LIM-domain binding protein Ldb1 and its partner LMO2 act as negative regulators of erythroid differentiation. Proc. Natl. Acad. Sci. USA **94:**13707–13712.
41. **Visvader, J. E., D. Venter, K. Hahm, M. Santamaria, E. Y. Sum, L. O'Reilly, D. White, R. Williams, J. Armes, and G. J. Lindeman.** 2001. The LIM domain gene LMO4 inhibits differentiation of mammary epithelial cells in vitro and is overexpressed in breast cancer. Proc. Natl. Acad. Sci. USA **98:**14452–14457.
42. **Wadman, I. A., H. Osada, G. G. Grutz, A. D. Agulnick, H. Westphal, A. Forster, and T. H. Rabbitts.** 1997. The LIM-only protein Lmo2 is a bridging molecule assembling an erythroid, DNA-binding complex which includes the TAL1, E47, GATA-1 and Ldb1/NLI proteins. EMBO J. **16:**3145–3157.
43. **Yamada, Y., R. Pannell, A. Forster, and T. H. Rabbitts.** 2000. The oncogenic LIM-only transcription factor Lmo2 regulates angiogenesis but not vasculogenesis in mice. Proc. Natl. Acad. Sci. USA **97:**320–324.
44. **Yamada, Y., A. J. Warren, C. Dobson, A. Forster, R. Pannell, and T. H. Rabbitts.** 1998. The T cell leukemia LIM protein Lmo2 is necessary for adult mouse hematopoiesis. Proc. Natl. Acad. Sci. USA **95:**3890–3895.